As_4S_4 role on the photoinduced birefringence of silver-doped chalcogenide thin films

Sandra Helena Messaddeq,[1,*] Olivier Boily,[1] Silvia Helena Santagneli,[2] Mohammed El-Amraoui,[1] and Younès Messaddeq[1,2]

[1]*Center for Optics, Photonics and Lasers, Laval University, 2375 de la Terrasse, Quebec City, QC, G1V 0A6, Canada*

[2]*Instituto de Química, UNESP, Araraquara, C.P. 355, CEP 14801-970, Araraquara, SP, Brazil*

[*]*sandra.messaddeq@copl.ulaval.ca*

Abstract: $Ag_X(As_{40}S_{60})_{100-X}$ thin films (x = 7, 15, 25, 50) were deposited on glass slides by a co-evaporation technique under a vacuum. Photoinduced birefringence was induced using light provided from a continuous argon-ion laser operating at 488 nm. We investigated the impact of silver concentration and laser power density. The thin films structural changes after irradiation were characterized by Raman spectroscopy, indicating that addition of Ag induces the breaking of sulfur ring units and favors the creation of Ag-S-Ag bridging bonds. During this process, AgS_3 pyramids and As_4S_4 molecules are formed, the latter being responsible for an increased photoinduced birefringence.

OCIS codes: (160.2750) Glass and other amorphous materials; (160.5335) Photosensitive materials; (260.1440) Birefringence; (300.6450) Spectroscopy, Raman; (310.6860) Thin films, optical properties.

References and links

1. V. G. Zhdanov, B. T. Kolomiets, V. M. Lyubin, and V. K. Malinovskii, "Photoinduced optical anisotropy in chalcogenide vitreous semiconducting films," Phys. Status Solidi, A Appl. Res. **52**(2), 621–626 (1979).
2. V. K. Tikhomirov, M. Barj, S. Turrell, J. Kobelke, N. Idrissi, M. Bouazaoui, M. Capoen, and A. B. Seddon, "Non-linear Raman effects and photodarkening in chalcogenide glass As_2S_3," Europhys. Lett. **76**(2), 312–317 (2006).
3. K. Tanaka, K. Ishida, and N. Yoshida, "Mechanism of photoinduced anisotropy in chalcogenide glasses," Phys. Rev. B Condens. Matter **54**(13), 9190–9195 (1996).
4. V. M. Lyubin and V. K. Tikhomirov, "Intrinsic and photoinduced elliptical dichroism and birefringence in glassy semiconductors," J. Non-Cryst. Solids **137–138**, 993–996 (1991).
5. C. V. Raman, "Structural birefringence in amorphous solids," Proc. Indian Acad. of Sci. A **31**(4), 207–212 (1950).
6. E. Márquez, J. B. Ramírez-Malo, J. Fernándes-Peña, P. Villares, R. Jiménez-Garay, P. J. S. Ewen, and A. E. Owen, "On the influence of Ag-photodoping on the optical properties of As-S glass films," J. Non-Cryst. Solids **164–166**, 1223–1226 (1993).
7. J. I. Masters, G. M. Goldberg, and J. M. Lavine, "Photographic Ag photodoping of amorphous As_2S_3 films," Electron. Device Lett. **1**(4), 61–62 (1980).
8. D. Nazarova, L. Nedelchev, P. Sharlandjiev, and V. Dragostinova, "Anisotropic hybrid organic/inorganic (azopolymer/SiO_2 NP) materials with enhanced photoinduced birefringence," Appl. Opt. **52**(22), E28–E33 (2013).
9. T. Kawaguchi, S. Maruno, and S. R. Elliott, "Photoinduced surface deposition of metallic silver in Ag-As-S glasses: effect of addition of other elements," J. Non-Cryst. Solids **212**(2-3), 166–172 (1997).
10. R. Swanepoel, "Determining refractive index and thickness of thin films from wavelength measurements only," J. Opt. Soc. Am. A **2**(8), 1339–1343 (1985).
11. K. Tanaka, M. Itoh, N. Yoshida, and M. Ohto, "Optical and electrical properties of Ag-As-S glasses," J. Appl. Phys. **77**(3), 1034–1039 (1995).
12. V. Ilcheva, P. Petkov, T. Petkova, and V. Boev, "Silver containing chalcogenide glasses and their applications,"presented at the Innovation Week on Renewable Energy Systems, Patras, Greece, 1–12 July 2012.
13. K. Palanjyan, S. H. Messaddeq, Y. Messaddeq, R. Vallée, E. Knystautas, and T. Galstian, "Study of photoinduced birefringence vs As content in thin Ge-As-S films," Opt. Mater. Express **3**(6), 671–683 (2013).
14. Y. Jun, M. Hai, Z. Jiang-Ying, W. Pei, L. Jian-Jing, L. Yong-Hua, L. Jian, and Z. Qi-Jin, "Effects of laser-induced heating on the photoinduced birefringence in azobenzene-side-chain copolymer," Chin. Phys. Lett. **20**(10), 1826–1828 (2003).

#257383 Received 15 Jan 2016; revised 24 Mar 2016; accepted 28 Mar 2016; published 4 Apr 2016

15. V. Boev, M. Mitkova, L. Nikolova, T. Todorov, and P. Sharlandjiev, "Photoinduced changes in the optical constants of Ge-Se-AgI thin films," Opt. Mater. **13**(4), 389–396 (2000).
16. M. Krbal, T. Wagner, T. Srba, J. Schwarz, J. Orava, T. Kohoutek, V. Zima, L. Benes, S. O. Kasap, and M. Frumar, "Properties and structure of $Ag_X(As_{0.33}S_{0.67})_{100-X}$ bulk glasses," J. Non-Cryst. Solids **353**(13–15), 1232–1237 (2007).
17. N. Yoshida and K. Tanaka, "Ag migration in Ag-As-S glasses induced by electron-beam irradiation," J. Non-Cryst. Solids **210**(2–3), 119–129 (1997).
18. M. Ohto and K. Tanaka, "Scanning tunneling spectroscopy of Ag-As-Se ion-conducting glasses," Appl. Phys. Lett. **71**(23), 3409–3411 (1997).
19. N. Choudhary and A. Kumar, "Dielectric relaxation in glassy $Se_{70}Te_{30-X}ag_X$," Indian J. Pure Appl. Phy. **44**(1), 62–65 (2006).
20. M. Popescu, "Disordered chalcogenide optoelectronic materials: phenomena and applications," J. Optoelectron. Adv. Mater. **7**(4), 2189–2210 (2005).
21. O. Matsuda, H. Oe, K. Inoue, and K. Murase, "Electronic and thermal processes during the photo-induced crystallization of amorphous $GeSe_2$," J. Non-Cryst. Solids **192–193**, 524–528 (1995).
22. T. Wagner, S. O. Kasap, M. Vleck, A. Sklenár, and A. Stronski, "Modulated-temperature differential scanning calorimetry and Raman spectroscopy studies of As_XS_{100-X} glasses," J. Mater. Sci. **33**(23), 5581–5588 (1998).
23. R. Holomb, V. Mitsa, P. Johansson, N. Mateleshko, A. Matic, and M. Veresh, "Energy-dependence of light-induced changes in g-$As_{45}S_{55}$ during recording the micro-Raman spectra," Chalcogenide Lett. **2**(7), 63–69 (2005).
24. F. Kyriazis and S. N. Yannopoulos, "Colossal photostructural changes in chalcogenide glasses: athermal photoinduced polymerization in As_XS_{100-X} bulk glasses revealed by near-bandgap Raman scattering," Appl. Phys. Lett. **94**(10), 101901 (2009).
25. W. Li, S. Seal, C. Rivero, C. Lopez, K. Richardson, A. Pope, A. Schulte, S. Myneni, H. Jain, K. Antoine, and A. C. Miller, "Role of S/Se ratio in chemical bonding of As-S-Se glasses investigated by Raman, X-ray photoelectron, and extended X-ray absorption fine structure spectroscopies," J. Appl. Phys. **98**(5), 053503 (2005).
26. A. Kovalskiy, M. Vleck, K. Palka, R. Golovchak, and H. Jain, "Wavelength dependence of photostructural transformations in As_2S_3 thin films," Phys. Procedia **44**, 75–81 (2013).
27. M. Ohta, "Effect of small amounts of silver on the electrical properties of As_2S_3 glasses," Phys. Status Solidi, A Appl. Res. **159**(2), 461–468 (1997).
28. I. T. Penfold and P. S. Salmon, "Glass formation and short-range order in chalcogenide materials: The $(Ag_2S)x(As_2S_3)_{1-x}$ ($0 \leq= X \leq= 1$) pseudobinary tie line," Phys. Rev. Lett. **64**(18), 2164–2167 (1990).
29. J. Tasseva, R. Todorov, T. Babeva, and K. Petkov, "Structural and optical characterization of Ag photo-doped thin $As_{40}S_{60-X}se_X$ films for non-linear applications," J. Opt. **12**(6), 065601 (2010).
30. K. Palka, T. Syrovy, S. Schröder, S. Brückner, M. Rothhardt, and M. Vleck, "Preperation of arsenic sulfide thin films for integrated optical elements by spiral bar coating," Opt. Mater. Express **4**(2), 384–395 (2014).
31. T. S. Kavetskyy, "Radiation-induced structural changes in chalcogenide glasses as revealed from Raman spectroscopy measurements," Semicond. Phys. Quantum Electron. & Optoelectron. **16**(1), 27–36 (2013).
32. K. E. Asatryan, B. Paquet, T. V. Galstian, and R. Vallée, "Phenomenological model of anisotropic microstructures in a-As_2S_3 chalcogenide glass," Phys. Rev. B **67**(1), 014208 (2003).
33. V. K. Tikhomirov, M. Barj, S. Turrell, J. Kobelke, N. Idrissi, M. Bouazaoui, B. Capoen, and A. B. Seddon, "Non-linear Raman effects and photodarkening in chalcogenide glass As_2S_3," Europhys. Lett. **76**(2), 312–317 (2006).
34. I. Kaban, P. Jóvári, T. Wagner, M. Frumar, S. Stehlik, M. Bartos, W. Hoyer, B. Beuneu, and M. A. Webb, "Atomic structure of As_2S_3-Ag chalcogenide glasses," J. Phys. Condens. Matter **21**(39), 395801 (2009).

1. Introduction

Chalcogenide glasses are well known to be light sensitive materials when illuminated by light having energy close to their bandgap energy. Their photoinduced properties allow a wide spectrum of physical and optical properties changes. Particularly, photo-induced anisotropy (PIA) induced by exposure to polarized light has been first reported by Zhdanov et al. more than 30 years ago [1]. Since then, extensive studies have been carried out to understand the PIA mechanisms. Nevertheless, they remain not well understood.

A large majority of the previous studies on photoinduced anisotropy have focused on As-S thin films of stoichiometric composition – namely, As_2S_3 – due to its good stability and its largest polarizability of all chalcogenide glasses [2]. In that case, photoinduced anisotropy was usually explained by the orientation of quasicrystalline clusters [3] or the re-orientation with polarized light of interatomic covalent bonds [4].

In this text, photoinduced birefringence (PIB) will accordingly refer to structural birefringence ; an optical characteristic exhibited by amorphous solids under special circumstances, originating from structural anisotropy [5].

#257383 Received 15 Jan 2016; revised 24 Mar 2016; accepted 28 Mar 2016; published 4 Apr 2016

Addition of silver in arsenic based chalcogenide thin films affects their bonding configuration, leading to a change in their electrical and optical properties. Also, it is well known that As-S-Ag materials exhibit interesting photoinduced phenomena mainly based on the motion of metal ions along the direction of the incoming irradiation [6,7]. Based on these facts, we can suppose that addition of silver could affect the bonding configuration and thus improve the PIB, since we would induce a photo-rearrangement or rotation of some new structural units.

The present work reports the compositional effect of Ag on the optical and structural properties of $As_{40}S_{60}$ chalcogenide thin films. In particular, the study of the dependence between PIB and silver amount reveals that the As-S-Ag thin film birefringence can be attributed to As_4S_4 molecules.

The ability to induce optical birefringence in an amorphous chalcogenide material provides a pathway to control the photoinduced polarization of light and could have a significant impact on the conception of optical elements.

2. Experimental

Glassy films of the binary system $As_{40}S_{60}$ and the ternary system $Ag_x(As_{40}S_{60})_{100-x}$ (x = 7, 15, 25, 50) were deposited by co-thermal evaporation from pure precursors, Ag element and $As_{40}S_{60}$ glass, onto microscope glass slides. A Nanochrome device (IntlVac), equipped with a current induced heated source and an electron beam evaporator was used.

The two sources were arranged in co-evaporation geometry, where the two vapor cones emanating from their respective source provided an area of overlap at the substrate, allowing deposition of ternary films homogeneous in thickness with dimensions of 5 x 8 cm. The substrate holder was placed at 30 cm above the heating source and the electron beam evaporator. The current induced heated source was used to evaporate Ag, whereas the electron beam was used to evaporate $As_{40}S_{60}$ glass. Before the deposition, the chamber was evacuated down to approximately 10^{-6} Pa. Deposition was carried at room temperature. The deposition rate and thickness of each element were automatically controlled with pre-calibrated quartz crystal monitors. During the process, the substrate holder was rotated at 80 rpm to improve film homogeneity.

By independently varying the evaporation rates of glassy $As_{40}S_{60}$ and metallic Ag, it was possible to deposit films with different compositions belonging to the As-S-Ag ternary system. The deposition rate of Ag varied between 0.5 and 4 $Å.s^{-1}$, and that of $As_{40}S_{60}$ was approximately fixed at 10 $Å.s^{-1}$. The produced films typical thickness was about 1 μm.

The chemical composition of the films was obtained by electron microprobe X-ray analyzes (EDAX) within an accuracy of ± 2 at.%.

The films optical transmittance in the range of 300 - 1100 nm was recorded with an UV-visible spectrophotometer (CARY 5000 from VARIAN). The transmittance spectra were used to measure the films band gap energy (Eg) and to evaluate their refractive index.

Raman spectra were recorded with a Renishaw inVia spectrometer coupled to a Leica DM2700 microscope. A back-scattering geometry was used in the frequency range of 100 - 600 cm^{-1}. The excitation light source was a vertically polarized He-Ne laser with a wavelength of 633 nm and a power of 17 mW. The laser beam was focused with a 50X long working distance objective, generating a sub-micron spot size containing a total power at the sample of approximately 5 - 10 mW. The frequency uncertainty was estimated to be ± 2 cm^{-1}. The deconvolution of Raman spectra was performed using the curve fit function of Wire 4.1 software.

Figure 1 shows the setup used to irradiate the samples. PIB was induced by the S-polarized beam of an Ar + laser operating at 488 nm. A Glan-Taylor prism (GT) was used to guarantee a linearly polarized excitation beam.

The reading beam was a low power CW He-Ne laser beam operating at 633 nm. Its polarization was aligned, by means of a half-wave plate (P), at 45° with respect to the polarization of the excitation beam. The two laser beams were aligned to overlap at the same

#257383 Received 15 Jan 2016; revised 24 Mar 2016; accepted 28 Mar 2016; published 4 Apr 2016

point on the sample (S). A second polarizer was placed after the sample in crossed configuration. The change in transmission of the probe beam was measured with a Newport dual-channel photodetector (D) (Model-2832c), and data was collected through Matlabview software.

Before irradiation, each film was optically isotropic and showed no transmittance. After irradiation with 488 nm linearly polarized light, a clearly homogeneous reorientation was obtained.

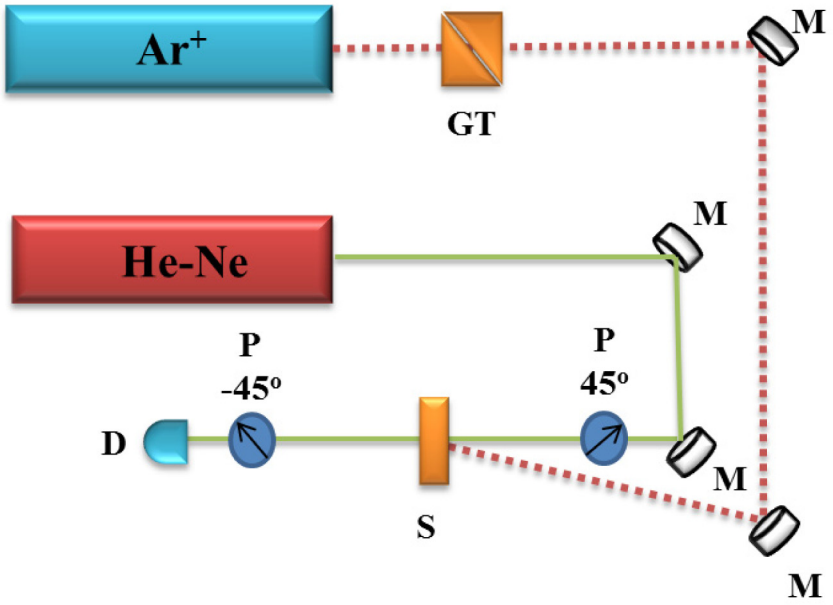

Fig. 1. Experimental set-up to measure photoinduced birefringence: Ar + and He-Ne lasers; S-Sample; M- Mirror; P-Polarizer; D- Photodetector; GT- Glan-Taylor Prism.

The photoinduced birefringence Δn could be determined by measuring the transmission of the reading laser $T = I/I_0$ according to:

$$\Delta n = \frac{\lambda}{\pi d} \sin^{-1}\left(\sqrt{\frac{I}{I_0}}\right) \quad (1)$$

where λ is the wavelength of the reading laser, d is the film thickness, I is the intensity of the incident light and I_0 is the light intensity after the Glan-Taylor prism [8].

3. Results and discussion

3.1 Characterization of the thin films properties

The elemental composition of $Ag_x(As_{40}S_{60})_{100-x}$ chalcogenide films was determined by energy dispersive X-ray analysis (EDAX) (see Table 1). The composition of the as-deposited $As_{40}S_{60}$ thin film was almost similar to that of the bulk glass. Through the co-evaporation process, we obtained films with an atomic percentage of silver between 7 and 50 at.%. It can be observed that the composition of some films is out of the standard amorphous region for the Ag-As-S glass system [9]. Nevertheless, obtained films were in a metastable amorphous state. The thin films amorphous nature was certified by XRD technique. Absence of sharp peaks, in the XRD spectra (Fig. 2), confirms that the deposited films were amorphous.

Optical transmission spectra are shown in Fig. 3 as a function of glass composition, for thin films with a thickness of 1.0 μm. They were used to determine refractive indices, with Swanepoel's method [10], and optical bandgaps (E_g), from Tauc's extrapolation procedure

#257383 Received 15 Jan 2016; revised 24 Mar 2016; accepted 28 Mar 2016; published 4 Apr 2016

(see Table 1). To perform Tauc's extrapolation procedure, the program PARAV-V1.0 was used.

Table 1. EDX analysis of $Ag_X(As_{40}S_{60})_{100-X}$ chalcogenide thin films

Sample	Element (at.%)			Optical bandgap (eV)	Refractive index @ 633 nm
	As	S	Ag		
$As_{40}S_{60}$ bulk glass	40	60	0	2.40	2.60
$As_{40}S_{60}$ thin film	42	58	0	2.38	2.80
$Ag_7(As_{40}S_{60})_{93}$	33	60	7	2.29	2.85
$Ag_{15}(As_{40}S_{60})_{85}$	32	53	15	2.17	2.90
$Ag_{25}(As_{40}S_{60})_{75}$	29	46	25	2.04	3.20
$Ag_{50}(As_{40}S_{60})_{50}$	21	29	50	1.72	3.50
$AgAsS_2$	25	50	25	2.10 [11]	-

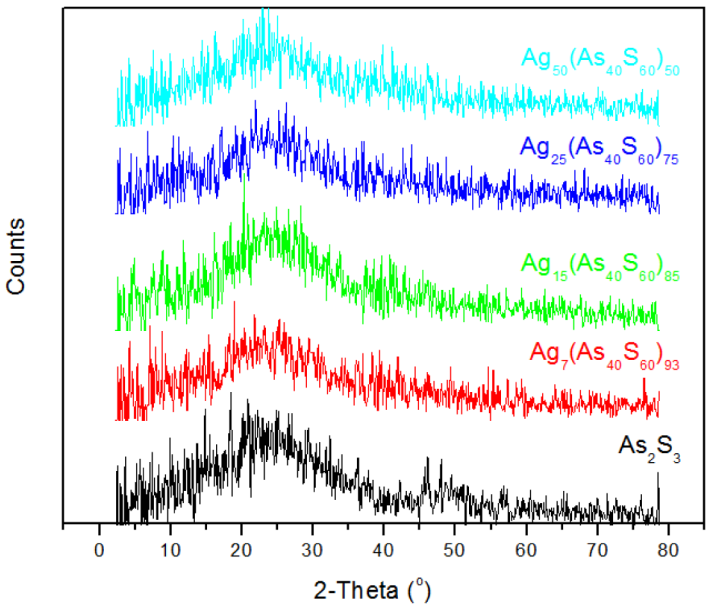

Fig. 2. XRD spectra of $Ag_X(As_{40}S_{60})_{100-X}$ chalcogenide thin films.

#257383 Received 15 Jan 2016; revised 24 Mar 2016; accepted 28 Mar 2016; published 4 Apr 2016

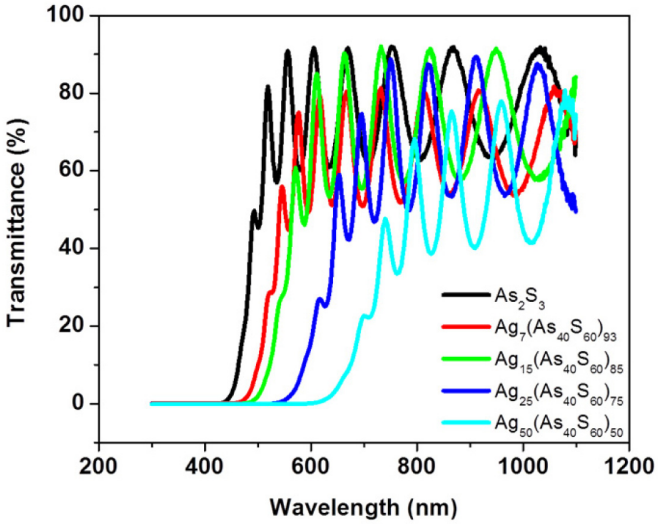

Fig. 3. Optical transmission spectra of $Ag_X(As_{40}S_{60})_{100-X}$ chalcogenide thin films.

A shift of the bandgap position is observed as the silver content is increased. The optical band gap decreases from 2.38 eV to 1.72 eV when the silver amount is increased from 0 to 50 at.%. This red shift of the absorption edge is probably caused by the formation of additional defect states localized just above the valence band, coming from the atomic substitution of As by Ag [12].

Refractive indices at 633 nm increase when silver amount is increased. This augmentation can be explained by the high polarizability of heavy atoms, such as silver. As a result, the optical density of the material increases.

3.2 Photoinduced birefringence

An experimental measurement of the typical behavior of PIB in chalcogenide As-S-Ag thin films is illustrated in Fig. 4. Note that while the writing laser is off, the transmission of the probe laser is null, which proves the isotropic orientation of the structures inside the thin films. From the moment that the writing laser is switched on, there is an abrupt increase in the transmission signal of the reading laser, showing the existence of PIB. Shortly after, depending on material composition and writing laser power density, this signal tends to saturate due to the equilibrium between the orientation and disorientation processes of molecules.

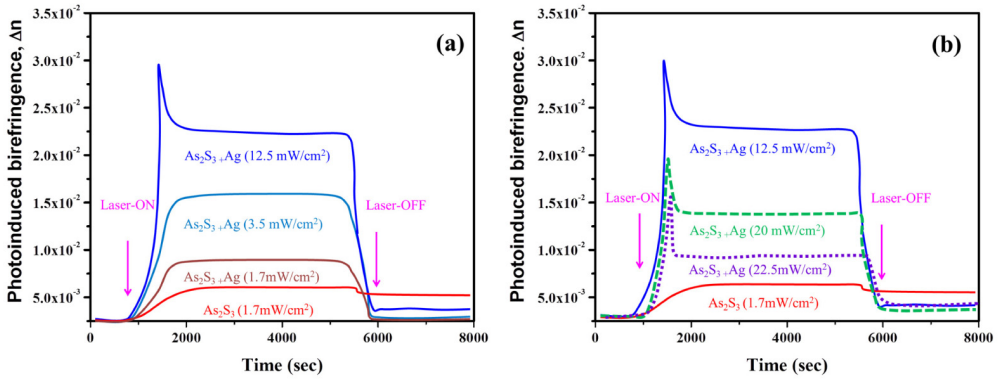

Fig. 4. Typical changes in the average refractive index of $As_{40}S_{60}$ and $Ag_{15}(As_{40}S_{60})_{85}$ thin films with time at low (a) and high (b) power densities.

#257383 Received 15 Jan 2016; revised 24 Mar 2016; accepted 28 Mar 2016; published 4 Apr 2016

Figure 4(a) shows the average refractive index change Δn for the samples $As_{40}S_{60}$ and $Ag_{15}(As_{40}S_{60})_{85}$ for three different power densities of the exciting Ar + beam (I = 1.7, 3.5 and 12.5 mW/cm^2). It is seen that the optical response is power dependent and that light with higher intensity initiates a larger increase of the birefringence signal.

The initial growth with time of PIB is often described by a bi-exponential equation: $\Delta n = A[1-\exp(-t/t_1)] + B[1-\exp(-t/t_2)]$ where t is time, t_1 and t_2 are time constants of processes appearing during excitation, and A and B are the amplitudes associated with these processes. The decay - or relaxation - of PIB can be defined by the same equation. Equation parameters are obtained with a curve fit of the experimental PIB curves.

The birefringence excitation process is dependent on writing laser power density. We observed in $Ag_{15}(As_{40}S_{60})_{85}$ thin films that the characteristic time (t_1) during excitation decreases (from about 1900 to 140 s) as the power density increases from 1.7 to 20 mW/cm^2. We can assume that the mobility of molecules increased and that the birefringence process consequently accelerated. A similar power density dependence was observed in Ge-based chalcogenide thin films [13].

Interestingly, we note that for higher power densities, the photoinduced refraction index change passes through a maximum. This behavior is only observed for samples in which silver has been added. The maximum refractive index change (Δn_{max}), measured in 15 at.% Ag-based films, reaches $3*10^{-2}$ at 12.5 mW/cm^2, rapidly decreases and then stabilizes at $2.3*10^{-2}$. Additional measurements show that PIB significantly decreases when laser power density is increased further between 20 and 22.5 mW/cm^2.

A PIB peak – as seen in the $Ag_{15}(As_{40}S_{60})_{85}$ sample exposed at 12.5 mw/cm^2 – was also reported in polymers and chalcogenide thin films, and was assigned to two different processes. In polymeric materials, the maximum observed intensity was related to the local thermal heating of the polymer caused by laser irradiation [14]. Otherwise, in Ge-Se chalcogenide thin films [15], the maximum change was assigned to two different mechanisms, each with a different rate. In the first process, charge carriers were created by light in the disordered Ge-Se network, allowing a displacement of the atoms. In the second process, a rearrangement of the bonds and the bond angles resulted in an average refractive index change with an opposite sign.

The surface temperature of the As-S-Ag samples was monitored during exposure using a thermal camera (Jenoptik, Variocam) with a close-up lens, which provides a spatial resolution of 50 μm. We observed that the temperature of the sample increased for higher power density exposures. For example, at a power density of 15 mW/cm^2, a temperature of 95 °C is reached after 10 seconds. Bearing in mind that in similar As-S-Ag glass compositions, the glass transition temperature is around 150 °C and the crystallization temperature around 240 °C [16], a rise of 95 °C is not sufficient to affect the thermal behavior of the thin films. In our case, we can thereby exclude the effect of laser heat accumulation as responsible for the maximum peak of photoinduced refraction index change. In the next section we will discuss the structural features involved in the PIB.

For thin films of $As_{40}S_{60}$, we note a partial relaxation of the PIB when the excitation beam is turned off, leaving a residual signal, as seen in Fig. 4. This indicates that the laser excitation produced oriented structures that are permanent (photo-orientation effect). However, as it can be observed in $Ag_{15}(As_{40}S_{60})_{85}$ thin films, the birefringence decays suddenly when the excitation beam is turned off. This means that the initial isotropic feature is reversible. We have performed additional tests (not reported here) showing that this reversibility can be repeated for several cycles (up to 5 times). This demonstrates the feasibility of optical storage in As-S-Ag thin films.

Figure 5 shows the influence of Ag content on PIB at different power densities. As can be seen, the birefringence signal increases as the amount of silver doped into the $As_{40}S_{60}$ thin film increases, reaching a maximum for 25% of Ag at 12.5 mW/cm^2. For $Ag_{25}(As_{40}S_{60})_{75}$ films, the maximal change in birefringence Δn is approximately $2.3*10^{-2}$. Such a value is rather high compared to other As-based chalcogenide materials [12,14]. However, it is worth mentioning that even if a higher value of PIB is obtained, the excitation time to achieve such a

#257383 Received 15 Jan 2016; revised 24 Mar 2016; accepted 28 Mar 2016; published 4 Apr 2016

molecular rearrangement is drastically increased (from about 40 to 3100 s) as we increase the amount of silver from 0 to 50 at.%. Even if higher values of PIB were obtained for the $Ag_{25}(As_{40}S_{60})_{75}$ sample, we further studied the $Ag_{15}(As_{40}S_{60})_{85}$ thin film, in which the PIB process is quite faster.

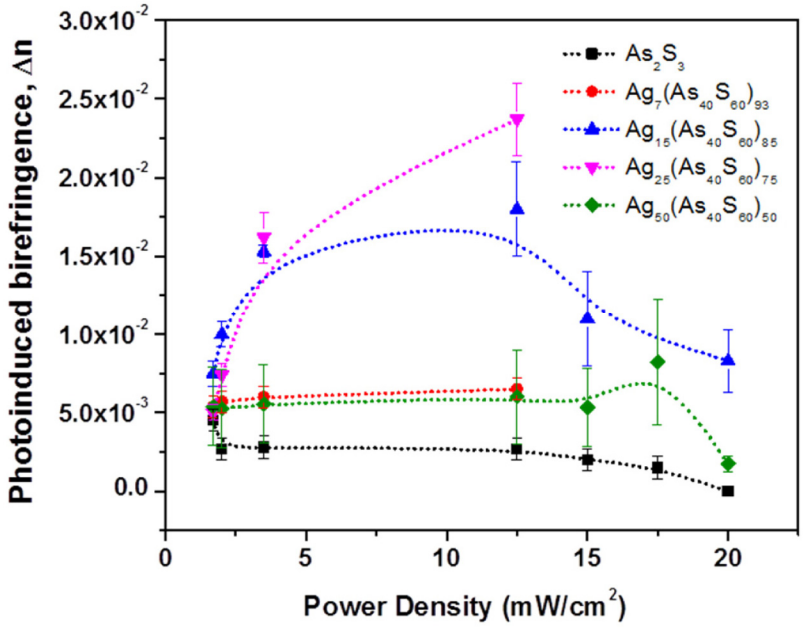

Fig. 5. Effect of silver amount and laser power density on PIB in $Ag_X(As_{40}S_{60})_{100-X}$ thin films.

It can be observed that PIB diminishes when laser power density is increased above 15 mW/cm^2 or with high silver content. This phenomenon can be associated with the migration of silver into the irradiated area. This migration has been confirmed by EDX measurements performed after irradiation (Table 2). These measurements indicate that, after 90 minutes of exposure, the silver amount in an irradiated area is up to three times higher in comparison to a non-irradiated area. It is well known that in silver chalcogenide films, silver migration is induced toward the irradiated region under light exposure [17,18]. According to Choudhary [19], since there are a large number of dangling bonds in chalcogenide glasses, one would eventually expect a new equilibrium to occur after migration, in which dipoles of Ag^+ coupled to dangling bonds would form, inducing a rearrangement of atomic structure. Popescu [20] indicates that the introduction of Ag into As_2S_3 glasses allows the extraction, upon exposure to intense light, of some arsenic atoms from the As_2S_3 network. The remaining sulfur atoms interact strongly with Ag and form a binary compound; Ag_2S. Similar results were found with $Se_{70}Ag_{15}I_{15}$ glasses, where photo-crystallization is accompanied by photoinduced anisotropy.

Table 2. EDX measurement of $Ag_{15}(As_{40}S_{60})_{85}$ thin films before and after irradiation at different times

Sample	Element (at.%)		
	As	S	Ag
Before irradiation	32	53	15
10 minutes	26	41	32
90 minutes	17	38	43

In our case, the power density increase or the silver amount increase in a silver-doped As_2S_3 thin film leads to a favored migration of silver into the exposed area and the formation

#257383 Received 15 Jan 2016; revised 24 Mar 2016; accepted 28 Mar 2016; published 4 Apr 2016

of acanthite (Ag_2S) crystals. These mechanisms result in a reduced PIB. A detailed explanation about the rearrangement of the structure will be discussed in the next section.

3.3 Morphological analysis

Figure 6 shows the micrographs of the $Ag_{15}(As_{40}S_{60})_{85}$ thin film surface topology after irradiation at 12.5 mW/cm^2 versus exposure time. A permanent modification of the morphology is observed.

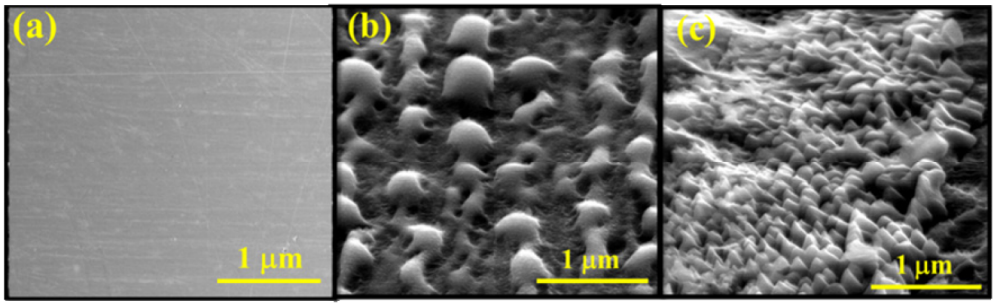

Fig. 6. SEM images of the $Ag_{15}(As_{40}S_{60})_{85}$ sample surface before irradiation (a) and after irradiation at 12.5 mW/cm^2, for (b) 10 minutes and (c) 90 minutes.

The laser beam spot is about 2 mm in diameter and its effect on the thin film surface morphology becomes more prominent with increasing exposure time. The irradiated region area gradually acquires a rough texture due to the appearance of small crystals (Fig. 6(b)). At longer exposure times (Fig. 6(c)), the morphology of the irradiated area change due to the formation of agglomerates of crystallites. The presence of crystallites of acanthite (Ag_2S) has been verified by XRD measurement.

Crystallization of amorphous chalcogenide glasses is induced by near or above bandgap-light. The photo-induced crystallization process occurs at temperatures lower than the thermal crystallization temperature. Electronic and thermal processes work cooperatively towards photo-crystallization, as shown in GeSe thin films [21].

3.4 Characterization of the photoinduced structural changes by Raman spectroscopy

Raman spectroscopy was used to investigate the $Ag_{15}(As_{40}S_{60})_{85}$ thin film structural changes after irradiation at different times and to explain the origin of PIB. In order to determine the basic vibrational modes that contribute to the Raman signal, spectra were analyzed in terms of convoluted peak functions by using a multiple curve fitting procedure of the experimental profiles into Gaussian functions.

Before discussing the effect of silver incorporation on photoinduced birefringence, it will be useful to keep in mind that the structure of As_2S_3 consists mainly of $AsS_{3/2}$ pyramidal units linked by As–S–As bridges. This structure was confirmed by several authors [22–24] and corresponds to the bands assigned at 310 (asymmetric stretching mode of $AsS_{3/2}$ pyramids), 345 (symmetric stretching vibrational mode of $AsS_{3/2}$ pyramids) and 380 cm^{-1} (As–S–As bridges). Additional bands are observed at 189 and 235 cm^{-1}, which have been associated to bending modes in As-As che bending of S_2As-AsS_2 in As_4S_4 (realgar) molecular units, respectively [23,25] (Fig. 7(a)).

Due to the incorporation of Ag in the $As_{40}S_{60}$ thin film matrix, a structural rearrangement is observed (Fig. 7(b)). The main bands associated with pyramidal units, i.e. at 315, 345 and 380 cm^{-1}, decrease while the appearance of an additional shoulder at 360 cm^{-1} is observed.

This new shoulder is assigned to As-As homopolar bonds containing structural units (such as As_4S_4 or As_4S_3) [26] which are formed only with silver addition. We should also note the increase of the vibrational modes at 189 and 235 cm^{-1}, demonstrating the formation of a large number of β-As_4S_4 structural units. The increase of As-As bonds due to the incorporation of silver in As_2S_3 glasses has already been reported by Ohta [27]. The author assumes that sulfur

#257383 Received 15 Jan 2016; revised 24 Mar 2016; accepted 28 Mar 2016; published 4 Apr 2016

atoms in As-S-As links are released during the dissociation of $AsS_{3/2}$ pyramids and form S-Ag-S bonds, simultaneously promoting the formation of As-As bonds. We have observed that such reorganizations produce the appearance of a new band at 375 cm^{-1} in the Raman spectrum which has been associated to S–Ag–S bonds connecting AgS_3 pyramidal units [28,29].

As the irradiation process begins (Figs. 7(c)-(d)), we can observe that the intensity of the band centered at 375 cm^{-1} grows systematically with irradiation time. The region associated with the As-As homopolar bonds increases drastically and the band associated with As_2S_3 pyramidal units disappears. The significant broadening of these bands (189, 235 and 360 cm^{-1}) in the Raman spectrum of doped silver chalcogenide thin films after irradiation was related to opened fragments of As_4S_4 cages, linked within the film matrix [30].

The irradiation of $Ag_{15}(As_{40}S_{60})_{85}$ thin films affects the bonding configuration by breaking the connection between sulfur and arsenic in pyramidal units. Sulfur atoms then create Ag-S-Ag bridging bonds to form $AgS_{3/2}$ pyramids. Furthermore, additional irradiation favors the dissociation of sulfur atoms in $As(S_{1/2})$ bonds, transforming AsS units into realgar As_4S_4 structures. The introduction of silver acts as a catalyst, promoting structural rearrangements to form As-As bonds in As_2S_3 chalcogenide thin films.

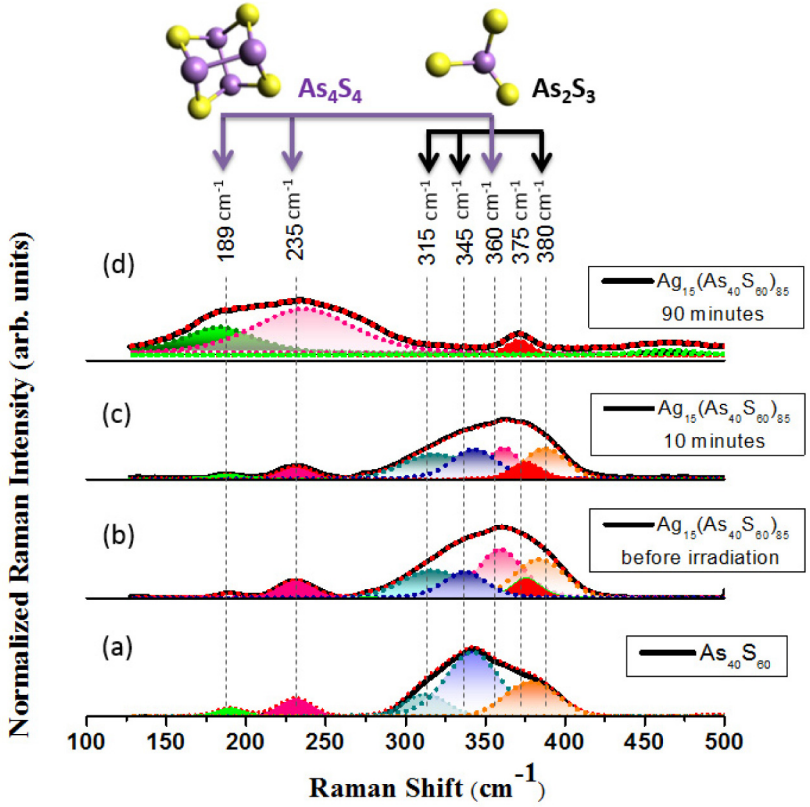

Fig. 7. Deconvoluted micro-Raman spectra of $As_{40}S_{60}$ and $Ag_{15}(As_{40}S_{60})_{85}$ thin films for different irradiation time. The arrows indicate the main bands corresponding to As_4S_4 molecules (purple arrows) and As_2S_3 pyramidal units (black arrows) observed before and after irradiation. As (●) and S (●).

Raman polarization dependence was also studied with a polarization setup, where the incident laser was polarized along the y axis. Polarized Raman was carried out in two configurations, namely; HH configuration, where incident laser light is polarized horizontally and Raman scattered signal analyzed horizontally; and HV configuration, where laser light

#257383 Received 15 Jan 2016; revised 24 Mar 2016; accepted 28 Mar 2016; published 4 Apr 2016

and Raman scattered signal are perpendicular to each other. The ratio of intensities I_{HV}/I_{HH} is defined as the depolarization ratio (ρ) and provides useful information about the symmetry of a vibrational mode.

In order to correlate the PIB with the symmetry of the scattering molecules we measured the depolarization ratio ($\rho = I_{HV}/I_{HH}$) of our thin film samples before and after irradiation (Fig. 8). This technique has been recently used by Kavetskyy to study the radiation-induced structural changes in chalcogenide glasses [31] and enables to distinguish Raman symmetrical modes from antisymmetrical modes.

A measured value of ρ that is equal to 0.75 is considered to indicate that the vibration under consideration doesn't have totally symmetric properties (i.e. it is not polarized), while values that are below 0.75 indicate that the vibration is totally symmetric.

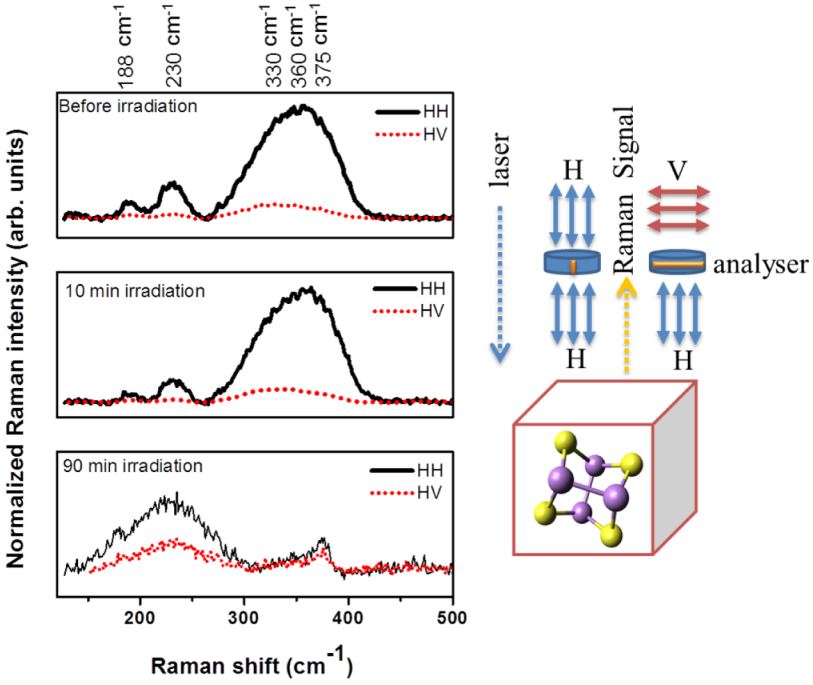

Fig. 8. Left side: HH and HV micro-Raman spectra of the $Ag_{15}(As_{40}S_{60})_{85}$ thin film before and after irradiation, for exposition times of 10 and 90 minutes, and a power density of 12.5 mW/cm^2 (optimized conditions for maximum PIB). Right side: A schematic representation indicating the polarization combinations in Raman measurements.

The principal feature determined from the Raman spectra is the monotonic increase of the depolarization ratio ρ of the bands (180, 235 and 360 cm^{-1}) associated with As_4S_4 molecules with increasing time of irradiation. Before illumination the depolarization ratio for As-As homopolar bonds ranges from 0.05 to 0.09. We thus conclude that the scattering bands are due to totally symmetric vibrations of As_4S_4. As we increase the exposure time up to 90 minutes, the calculated value of the depolarization ratio increases up to a value of 0.4. This indicates the transformation of a highly symmetric molecule to an asymmetric configuration, which denotes the polarized character of the bands after exposure.

From the above results shown by Raman measurements, we can correlate the increase in PIB in As_2S_3 chalcogenide thin films with the increased formation of As_4S_4 realgar molecular units, which is promoted by the addition of silver.

The role of As_4S_4 on PIA has already been suggested by Asatryan et al. To account for their experimental results, Asatryan has shown that the structures responsible for PIA in amorphous As_2S_3 thin films must have a disklike polarizability tensor [32]. The author proposes that As_4S_4 molecules are a suitable candidate to explain photoinduced anisotropy by

#257383 Received 15 Jan 2016; revised 24 Mar 2016; accepted 28 Mar 2016; published 4 Apr 2016

polarized light. Indeed, As_4S_4 units have a cagelike structure, which includes two planar homopolar As-As wrong bonds that are heavily polarized. Thus, the As_4S_4 polarizability tensor is ellipsoidal, being slightly flat at its poles, i.e. disklike. We can confirm this model, wherein As_4S_4 structures are responsible for PIB.

Polarized Raman measurements of As_2S_3 glasses specifically show that the band around 235 cm^{-1}, which is associated with realgar units, is polarized [33]. These units are responsible for PIB and their formation is promoted by the introduction of Ag. Silver induces the dissociation of S-S chains in behalf of the formation of $AgS_{3/2}$ pyramids. Sulfur atoms in remaining As-S-As links are eliminated, resulting in the formation of As-As bonds [34] (Figs. 9(a)-(b)). In Ag-doped thin films, the number of As_4S_4 molecules, and thereby the number of polarized As-As bonds, drastically increases. Ag-doped chalcogenide materials possess a high PIB value when compared to other As-based chalcogenides, owing to their large number of As_4S_4 units. Laser irradiation causes these units to bend and to orient themselves in a common direction which minimizes absorption (Fig. 9(c)). This rearrangement is promoted by the high flexibility of sulfur atoms and is suppressed in absence of irradiation (Fig. 9(d)). Indeed, aligned As_4S_4 molecules in the illuminated region tend to return to their original random arrangement when the writing laser is turned off. This phenomenon could explicate the fast decay of PIB. However, in As_2S_3 thin films, a certain amount of As_4S_4 molecules remain aligned, even when the laser is turned off. A residual birefringence is still observed.

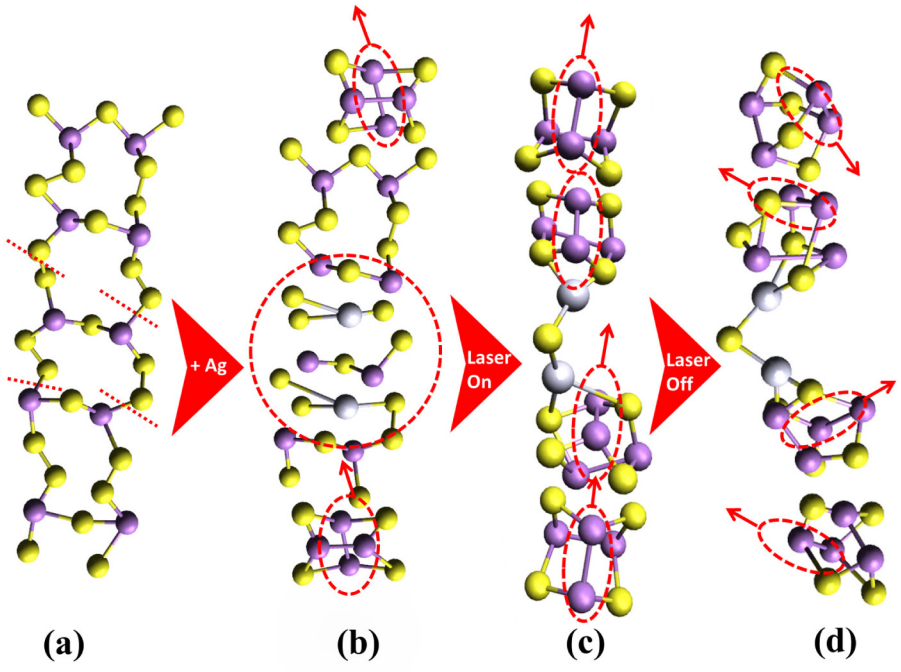

Fig. 9. (a) Schematic illustration of the As_2S_3 thin film structure. (b) Effect of silver doping. Photoinduced alignment of As-As homopolar bonds when the writing laser is turned on (c) and its annulment when the writing laser is turned off (d). The thin film isotropic feature is seen to be reversible. As (●), S (●), and Ag (●).

4. Conclusion

$Ag_x(As_{40}S_{60})_{100-x}$ thin films have been prepared by co-evaporation method. This method enlarges the vitreous domain, allowing a wide range of new metastable compositions.

Incorporation of Ag into the $As_{40}S_{60}$ thin film matrix induces a structural rearrangement favoring the appearance of $AgS_{3/2}$ pyramids and As_4S_4 molecules in detriment of $AsS_{3/2}$ pyramidal units. It has been shown that the $Ag_x(As_{40}S_{60})_{100-x}$ thin film PIB is dependent on

#257383 Received 15 Jan 2016; revised 24 Mar 2016; accepted 28 Mar 2016; published 4 Apr 2016

composition and laser power. Furthermore, PIB is reversible in silver doped chalcogenide thin films. From a structural point of view, it has been observed that the increase in PIB is due to the increase of As_4S_4 units. Laser irradiation preferentially causes As-As bonds that are parallel to the electric vector of the polarized light to reorient themselves in a direction that minimizes absorption, thus inducing a high PIB value (Δn).

Acknowledgments

This research was supported by the Natural Sciences and Engineering Research Council of Canada (NSERC), the Canada Foundation for Innovation (CFI), the Canada Excellence Research Chair in Photonic Innovations (CERCPI), the Ministère du Développement économique, de l'Innovation et de l'Exportation (MDEIE) and the Fonds de recherche du Québec - Nature et technologies (FRQNT).

#257383 Received 15 Jan 2016; revised 24 Mar 2016; accepted 28 Mar 2016; published 4 Apr 2016